

# Texture Reformer: Towards Fast and Universal Interactive Texture Transfer

Zhizhong Wang, Lei Zhao\*, Haibo Chen, Ailin Li,  
Zhiwen Zuo, Wei Xing\*, Dongming Lu

College of Computer Science and Technology, Zhejiang University  
{endywon, cszhl, cshbchen, liailin, zzwcs, wxing, ldm}@zju.edu.cn

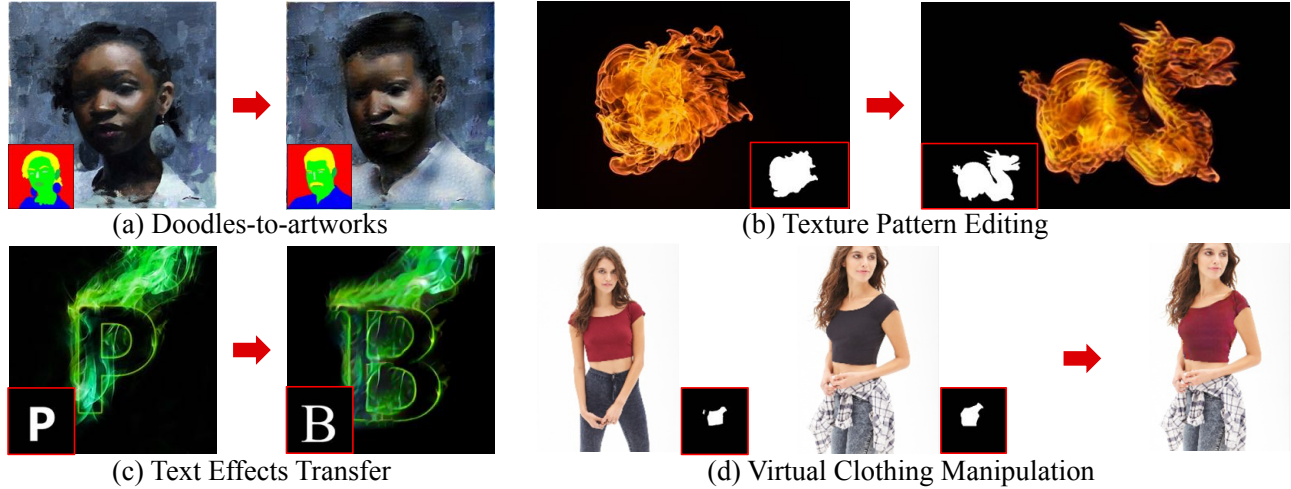


Figure 1: Representative results generated by our interactive texture reformer. The stylized images are synthesized under the guidance of corresponding user-specified semantic maps. Our framework is universal for multiple challenging user-controlled texture transfer tasks, *e.g.*, (a) turning doodles into artworks, (b) editing texture patterns, (c) transferring text effects, (d) manipulating clothing textures and distributions. Compared with the state-of-the-art interactive texture transfer algorithms, *it not only can achieve higher quality results but, more remarkably, also is 2-5 orders of magnitude faster.*

## Abstract

In this paper, we present the *texture reformer*, a fast and universal neural-based framework for interactive texture transfer with user-specified guidance. The challenges lie in three aspects: 1) the diversity of tasks, 2) the simplicity of guidance maps, and 3) the execution efficiency. To address these challenges, our key idea is to use a novel feed-forward multi-view and multi-stage synthesis procedure consisting of I) a global view structure alignment stage, II) a local view texture refinement stage, and III) a holistic effect enhancement stage to synthesize high-quality results with coherent structures and fine texture details in a coarse-to-fine fashion. In addition, we also introduce a novel learning-free *view-specific texture reformation (VSTR)* operation with a new semantic map guidance strategy to achieve more accurate semantic-guided and structure-preserved texture transfer. The experimental results on a variety of application scenarios demonstrate the effectiveness and superiority of our framework. And compared with the state-of-the-art interactive texture transfer algorithms, it not only achieves higher quality results but, more

remarkably, also is 2-5 orders of magnitude faster. Code is available at <https://github.com/EndyWon/Texture-Reformer>.

## 1 Introduction

As a variant of texture synthesis, texture transfer is a long-standing problem that seeks to transfer the stylized texture from a given sample to the target image (Efros and Freeman 2001). After the rapid development in recent years, a bunch of conventional (Hertzmann et al. 2001) or neural-based (Gatys, Ecker, and Bethge 2016) methods have been proposed and obtained visually appealing results. However, due to the lack of user guidance, general texture transfer methods often produce unsatisfying results against human expectations. To resolve this dilemma, the community resorts to using the user-specified semantic maps to guide the transfer process, which is called *interactive texture transfer* (Men et al. 2018). Users can control the shape, scale, and spatial distribution of the objects to be synthesized in the target image via semantic maps.

At first, the interactive texture transfer methods are only designed for specific usage scenarios. (Champandard 2016) proposed Neural Doodle to turn doodles painted by users into fine artworks with provided samples. Lu *et al.* designed

\*Corresponding authors.

HelpingHand (Lu et al. 2012), RealBrush (Lu et al. 2013), and DecoBrush (Lu et al. 2014) to edit different kinds of texture patterns. (Yang et al. 2017, 2019) achieved text effects transfer that can migrate various fantastic text effects of stylized texts onto raw plain texts. (Han et al. 2018) introduced an image-based virtual try-on network to transfer a target clothing item in a product image to the corresponding region of a clothed person. These approaches seem to be isolated, but they all share a common notion of transferring textures under user guidance.

To unify them, (Men et al. 2018) proposed a common framework for interactive texture transfer by incorporating multiple custom channels to dynamically guide the synthesis. This method is capable of handling various challenging tasks and achieves the state of the art. However, it relies on several CPU-based operations and a backward optimization process, thus usually requiring several minutes to generate a result for each interaction, which is prohibitively slow. Therefore, existing algorithms are hard to satisfy the practical requirements due to the limitations of efficiency or application scenarios. A fast and universal framework is eagerly desired, and it will undoubtedly improve the user experience and bring higher application and research value to both industry and academia.

However, achieving such a goal is a rather challenging task. The challenges mainly lie in three aspects: 1) The diversity of tasks: the discrepancies between different tasks make the transfer problem difficult to model uniformly. Besides, for each task, the algorithm should be robust to different input samples. 2) The simplicity of guidance maps: the doodle semantic map as guidance gives few hints on how to place different inner textures and preserve local high-frequency structures (Men et al. 2018). 3) The execution efficiency: the trade-off between efficiency and quality is always an intractable problem. This is particularly important for interactive systems since the insufficient computational speed not only brings inconvenience to users but also hampers the truly exploratory use of these techniques.

To address these challenges, in this paper, we propose the *texture reformer*, a fast and universal neural-based framework for interactive texture transfer with user-specified guidance. The key insight is to use a novel feed-forward multi-view and multi-stage synthesis procedure, which consists of three different stages: I) a global view structure alignment stage, II) a local view texture refinement stage, and III) a holistic effect enhancement stage. Specifically, for stage I and II, we introduce a novel *View-Specific Texture Reformation (VSTR)* operation with a new semantic map guidance strategy to achieve more accurate semantic-guided and structure-preserved texture transfer. By specifying a global view for VSTR, our stage I first captures and aligns the inner structures of the source textures as completely as possible. Then, the results are carefully rectified and refined in stage II via specifying a local view for VSTR. Finally, in stage III, we leverage the Statistics-based Enhancement (SE) operations to further enhance the low-level holistic effects (e.g., colors, brightness, and contrast). Note that our framework is built upon several auto-encoder networks trained solely for image reconstruction, and the VSTR and SE oper-

ations are *learning-free*. Therefore, it can achieve interactive texture transfer universally. By cascading the above three stages, our texture reformer can synthesize high-quality results with coherent structures and fine texture details in a coarse-to-fine fashion. We demonstrate the effectiveness and superiority of our framework on a variety of application scenarios, including doodles-to-artworks, texture pattern editing, text effects transfer, and virtual clothing manipulation (see Fig. 1). The experimental results show that compared with the state-of-the-art algorithms, our texture reformer not only achieves higher quality results but, more remarkably, also is 2-5 orders of magnitude faster. *As far as we know, our work is the first to meet the requirements of quality, flexibility, and efficiency at the same time in this task.*

In summary, our contributions are threefold:

- We propose a novel multi-view and multi-stage neural-based framework, *i.e.*, *texture reformer*, to achieve fast and universal interactive texture transfer for the first time.
- We also introduce a novel learning-free *view-specific texture reformation (VSTR)* operation with a new semantic map guidance strategy, to realize more accurate semantic-guided and structure-preserved texture transfer.
- We apply our framework to many challenging interactive texture transfer tasks, and demonstrate its effectiveness and superiority through extensive comparisons with the state-of-the-art (SOTA) algorithms.

## 2 Related Work

**Conventional Texture Transfer.** Conventional texture transfer relies on hand-crafted algorithms (Haerberli 1990) or features (Kwatra et al. 2005) to migrate the textures from source samples to target images. The pioneering works of (Efros and Leung 1999; Efros and Freeman 2001) sampled similar patches to synthesize and transfer textures. Later, (Hertzmann et al. 2001) proposed Image Analogy to generate the stylized result of the target image. (Barnes et al. 2009, 2010) proposed PatchMatch to accelerate the nearest-neighbor search process, which was further extended to image melding (Darabi et al. 2012), style transfer (Frigo et al. 2016), and text effects transfer (Yang et al. 2017), *etc.* However, for interactive texture transfer, these methods fail to synthesize the textures with salient structures and are prone to wash-out effects (Men et al. 2018). To combat the issues, (Men et al. 2018) proposed a common framework for interactive texture transfer by utilizing an improved PatchMatch and multiple custom channels to dynamically guide the synthesis, achieving SOTA performance. However, as analyzed in Sec. 1, this method suffers from rather slow computational speed, thus cannot satisfy the practical requirements.

Unlike the SOTA conventional texture transfer methods (Yang et al. 2017; Men et al. 2018), our proposed texture reformer is neural-based, and not only can achieve higher quality results but also is several orders of magnitude faster.

**Neural-based Style Transfer.** The seminal works of (Gatys, Ecker, and Bethge 2016, 2015) have proved the power of Deep Convolutional Neural Networks (DCNNs) (Simonyan and Zisserman 2014) in style transfer and texture synthesis, where the Gram matrices of the features

extracted from different layers of DCNNs are used to represent the style of images. Further works improved it in many aspects, including efficiency (Johnson, Alahi, and Fei-Fei 2016; Ulyanov et al. 2016), quality (Sheng et al. 2018; Jing et al. 2018; Gu et al. 2018; Kolkin, Salavon, and Shakhnarovich 2019; Park and Lee 2019; Wang et al. 2020b, 2021; Chen et al. 2020, 2021b,a; Lin et al. 2021; Cheng et al. 2021; An et al. 2021), generality (Li et al. 2017; Huang and Belongie 2017; Lu et al. 2019; Zhang, Zhu, and Zhu 2019; Jing et al. 2020), and diversity (Wang et al. 2020a; Chen et al. 2021c). For interactive style transfer, (Gatys et al. 2017) introduced user spatial control into (Gatys, Ecker, and Bethge 2016), which is further accelerated by (Lu et al. 2017). However, due to the characteristics of Gram matrix matching, these methods often produce disordered textures, which cannot preserve the local inner structures, as will be demonstrated in later Sec. 4.3.

Another line of neural-based style transfer is based on neural patches. (Li and Wand 2016a,b) first achieved it by combining Markov Random Fields (MRFs) and DCNNs. (Liao et al. 2017) proposed Deep Image Analogy for more accurate semantic-level patch matching. Later, (Chen and Schmidt 2016) leveraged a “style swap” operation for fast patch-based stylization. To incorporate user control, (Champandard 2016) augmented (Li and Wand 2016a) with semantic annotations, leading to higher quality and avoiding common glitches. However, the results usually contain too many low-level noises. Also, efficiency is concerned as it still relies on a time-consuming backward optimization process.

Generative Adversarial Networks (GANs) (Goodfellow et al. 2014) provide another idea to generate textures by training discriminator and generator networks to play an adversarial game. cGANs (Mirza and Osindero 2014), which were further extended to image-to-image translation (Isola et al. 2017), have been applied to many image manipulation tasks, such as interactive image editing (Zhu et al. 2016), texture synthesis (Frühstück, Alhashim, and Wonka 2019), sketch2image (Chen and Hays 2018), and inpainting (Zhao et al. 2020), etc. However, all of them are trained on class-specific datasets. By contrast, our method only needs one exemplar for generating the target image from a corresponding semantic map. Recently, some single image generative models (Shaham, Dekel, and Michaeli 2019; Lin et al. 2020) were also proposed to generate images based on only a single image. Nevertheless, these methods often produce poor results for images with complex texture details and structures, and need several hours to train the model on each pair of image samples.

### 3 Proposed Approach

We first describe the task of interactive texture transfer following the definitions in (Men et al. 2018). As illustrated in the left part of Fig. 3, given a stylized source image  $S_{sty}$  and its corresponding semantic map  $S_{sem}$ , interactive texture transfer aims to generate the stylized target image  $T_{sty}$  with a user-specified target semantic map  $T_{sem}$ . Users can control the shape, scale, and spatial distribution of the objects to be synthesized in the target image via semantic maps.

Using a semantic map that contains few hints to repro-

duce the structural image is a challenging task. The key challenge is to preserve the structures of the inner textures of each semantic region, *e.g.*, the clothing structures in the blue region of Fig. 3. (Men et al. 2018) combat it by introducing structure guidance based on the boundary patches of semantic maps to provide a prior in the synthesis procedure. However, it involves several structure extraction (Goferman, Zelnik-Manor, and Tal 2011) and propagation (Myronenko and Song 2010; Bookstein 1989) processes, which are cumbersome and time-consuming. In a fundamentally different way, we do not use any additional structure guidance but only benefit from the strong representative power of DCNNs to extract the multi-level image features. Based on these features, our key insight is to use a multi-view and multi-stage synthesis procedure to progressively generate structural textures in a coarse-to-fine fashion. In the following sections, we will first depict the overall pipeline and some critical components of our framework (Sec. 3.1), and then introduce each of its stages in detail (Sec. 3.2-3.4).

#### 3.1 Overview of Texture Reformer

The overall pipeline of our framework is depicted in Fig. 2, which consists of three stages: I) a global view structure alignment stage, II) a local view texture refinement stage, and III) a holistic effect enhancement stage. Specifically, stage I is similar to a global copy-and-paste, which roughly aligns the spatial positions of the source patterns in  $S_{sty}$  to the target positions in the target semantic map  $T_{sem}$ . This global view alignment can help preserve the inner structures of the source patterns as completely as possible, which is critical to synthesize the structure-preserved textures. The warping and finer alignment is achieved via stage II, which uses a rather small local view, and can rectify and refine the results of stage I to a large extent, thus robust for different deformation requirements. Finally, the low-level holistic effects (*e.g.*, colors, brightness, and contrast) are further enhanced in stage III, thereby obtaining high-quality results. The visualizations of the inputs/outputs of each stage are shown in Fig. 2 ( $T_{sty}^5 - T_{sty}$ ). These stages are carried out at different levels of VGG (Simonyan and Zisserman 2014) features and are hierarchically cascaded to work in a coarse-to-fine fashion. Uniformly, they share the same workflow that generates the outputs using an AE (auto-encoder)-based image reconstruction process coupled with bottleneck feature operations. We adopt view-specific texture reformation (VSTR) for stage I and II, and statistics-based enhancement (SE) for stage III, which we will introduce in detail.

**AE-based Image Reconstruction.** We construct auto-encoder networks for general image reconstruction. We employ the first parts (up to  $ReluX_{.1}$ ) of a pre-trained VGG-19 (Simonyan and Zisserman 2014) as encoders, *fix* them and train symmetrical decoder networks with the nearest neighbor interpolation as upsampling layers for inverting the bottleneck features to the original RGB images. As shown in Fig. 2, in our framework, we select feature maps at five layers, *i.e.*,  $ReluX_{.1}$  ( $X=1,2,3,4,5$ ), and train five decoders accordingly with the following loss:

$$\mathcal{L}_{recon} = \| I_r - I_i \|_2^2 + \lambda \| \Phi(I_r) - \Phi(I_i) \|_2^2 \quad (1)$$

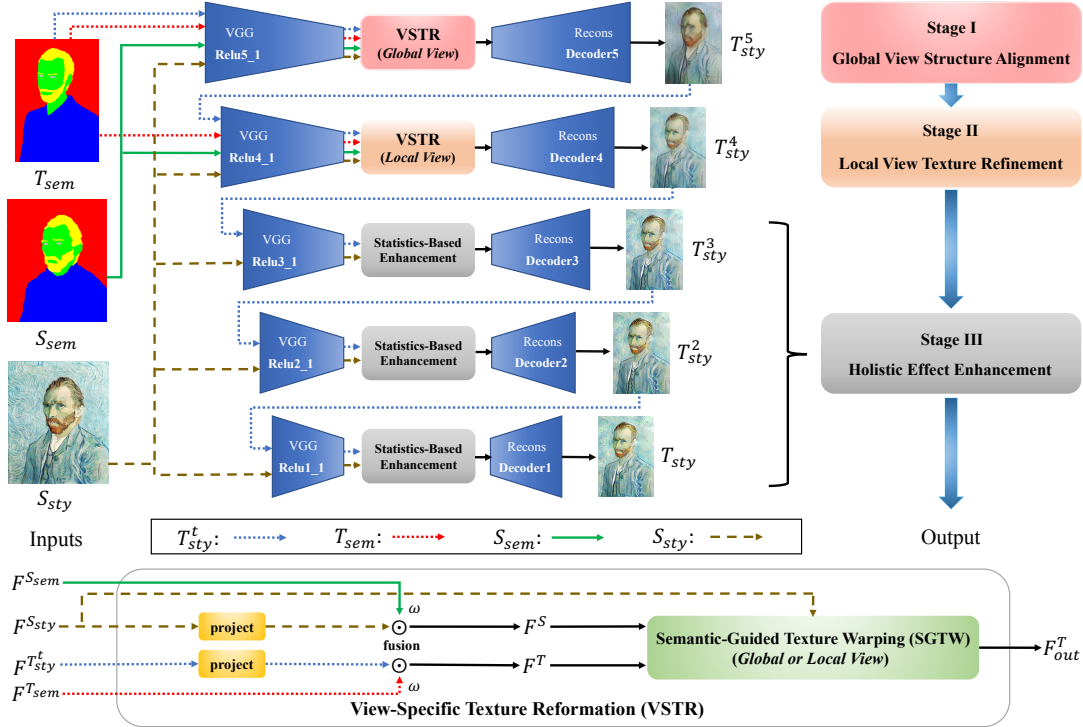


Figure 2: Overall pipeline of our proposed multi-view and multi-stage texture reformer.

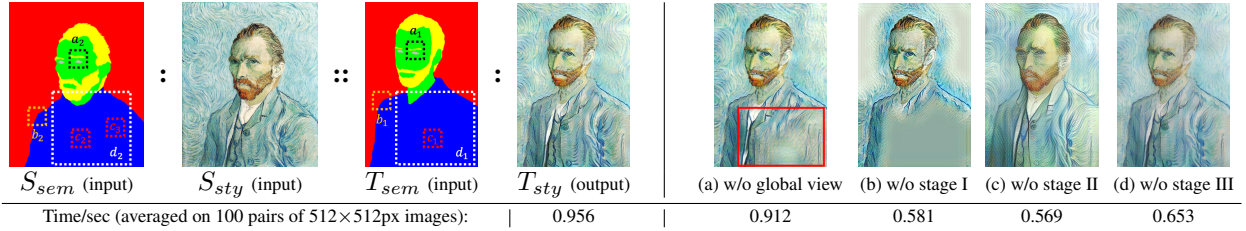


Figure 3: **Left:** Illustration of the interactive texture transfer task. Input three images:  $S_{sem}$  (semantic map of source image),  $S_{sty}$  (stylized source image aligned to  $S_{sem}$ ), and  $T_{sem}$  (user-specified semantic map of target image), the stylized target image  $T_{sty}$  with the style of source image  $S_{sty}$  can be automatically synthesized such that  $S_{sem} : S_{sty} :: T_{sem} : T_{sty}$ . **Right:** Effects of different critical components and stages in our texture reformer (Fig. 2). **Bottom:** Efficiency comparison.

where  $I_i$  and  $I_r$  are the input image and reconstructed output, and  $\Phi$  is the VGG encoder that extracts the  $ReluX_1$  features. The decoders are trained on the Microsoft COCO dataset (Lin et al. 2014) and  $\lambda$  is set to 1.

**View-Specific Texture Reformation (VSTR).** We propose a novel *learning-free* VSTR operation to robustly propagate the thorough texture patterns onto the target features under the guidance of semantic maps. Denote  $F^{S_{sty}}$  and  $F^{T_{sty}^t}$  as the VGG features (e.g., extracted from  $Relu5_1$ ) of the stylized source image  $S_{sty}$  and the temporary stylized target image  $T_{sty}^t$ . We first project them into a common space to standardize the data and dispel the domain gap,

$$F_1^{S_{sty}} = \frac{F^{S_{sty}} - \mu(F^{S_{sty}})}{\sigma(F^{S_{sty}})}; F_1^{T_{sty}^t} = \frac{F^{T_{sty}^t} - \mu(F^{T_{sty}^t})}{\sigma(F^{T_{sty}^t})}, \quad (2)$$

where  $\mu$  and  $\sigma$  are the mean and standard deviation.

Then, we fuse the information from the source and tar-

get semantic maps  $S_{sem}$  and  $T_{sem}$  to guide the propagations between corresponding semantic regions. Existing works (Chamandard 2016; Gatys et al. 2017) often directly concatenate the downsampled semantic maps, like follows:

$$F^S = F_1^{S_{sty}} \parallel \omega S_{sem}^l; F^T = F_1^{T_{sty}^t} \parallel \omega T_{sem}^l, \quad (3)$$

where  $\parallel$  denotes channel-wise concatenation.  $l$  denotes the downsampling factor.  $\omega$  is the hyperparameter that controls the weight of semantic awareness. However, as pointed out by (Gatys et al. 2017), this method has limited capacity to model complex textures and usually produces inaccurate semantic matching (e.g., the 2<sup>nd</sup> column in Fig. 4). This can be attributed to the information discrepancy between the RGB images and deep VGG features. In addition, the difference in the amount of channels may also make it hard to find a good compromise (i.e., the proper value of  $\omega$ ) between them.

To resolve this issue, we introduce a new semantic map guidance strategy in our VSTR. That is, first extracting the

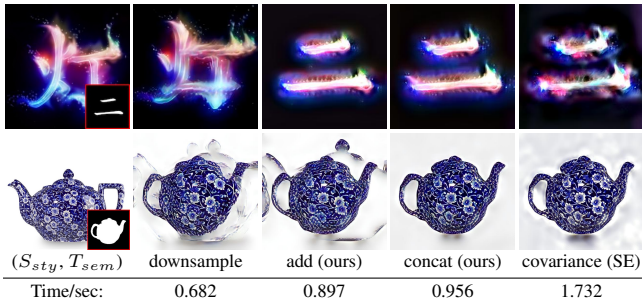


Figure 4: Comparison of different semantic map guidance strategies (2<sup>nd</sup> to 4<sup>th</sup> columns) and different enhancement operations (last column).

VGG features  $F^{S_{sem}}$  and  $F^{T_{sem}}$  for semantic maps  $S_{sem}$  and  $T_{sem}$ , and then conducting the fusion in the VGG embedding space.

$$F^S = F_1^{S_{sty}} \odot \omega F^{S_{sem}}; F^T = F_1^{T_{sty}} \odot \omega F^{T_{sem}}, \quad (4)$$

where the fusion operation  $\odot$  can be channel-wise concatenation or position-wise addition. We find these two operations could perform closely in some cases (e.g., the 3<sup>rd</sup> and 4<sup>th</sup> top images in Fig. 4). But in general, concatenation often achieves more accurate semantic guidance (see the 3<sup>rd</sup> and 4<sup>th</sup> bottom images in Fig. 4) yet addition can provide faster speed (see the bottom efficiency comparison in Fig. 4).

After obtaining the fused features  $F^S$  and  $F^T$ , inspired by (Chen and Schmidt 2016), we introduce a *Semantic-Guided Texture Warping (SGTW)* module with a specific field of view (i.e., patch size  $p$ ) to warp and transfer the textures. The detailed procedure is as follows:

1. Extract a set of  $p \times p$  original source patches from the original source feature  $F^{S_{sty}}$ , denoted by  $\{\phi_i(F^{S_{sty}})\}_{i \in \{1, \dots, n_s\}}$ , where  $n_s$  is the number of extracted patches.
2. Extract a set of  $p \times p$  fused source patches from the fused source feature  $F^S$ , denoted by  $\{\phi_i(F^S)\}_{i \in \{1, \dots, n_s\}}$ .
3. Determine the closest-matching fused source patch for each fused target patch in  $F^T$  by using a convolutional layer with the normalized fused source patches  $\{\phi_i(F^S) / \|\phi_i(F^S)\|\}$  as filters and  $F^T$  as input. The computed result  $\mathcal{T}$  has  $n_s$  feature channels, and each spatial location is a cosine similarity vector between a fused target patch and all fused source patches.
4. Binarizing the scores in  $\mathcal{T}$  such that the maximum value along the channel is  $\mathbf{1}$  and the rest are  $\mathbf{0}$ . The result is denoted as  $\hat{\mathcal{T}}$ .
5. Generate the output  $F_{out}^T$  by a deconvolutional layer with the original source patches  $\{\phi_i(F^{S_{sty}})\}$  as filters and  $\hat{\mathcal{T}}$  as input.

The novel insight behind SGTW is that we exploit the semantic-guided matching relationship between the patches of fused features  $F^S$  and  $F^T$  to reassemble and warp the original source feature  $F^{S_{sty}}$ . This not only guarantees the accurate alignment with the target semantic map, but also theoretically ensures that the output feature  $F_{out}^T$  can preserve the texture details of the original source feature  $F^{S_{sty}}$  losslessly, since all its patches are from  $F^{S_{sty}}$ . Moreover, by specifying different views for SGTW, we can control the granularity of preserved texture details (e.g., the integrity of inner structures) and the alignment accuracy with the target semantic map, as will be shown in later Sec. 3.2 and 3.3. By

leveraging SGTW, our VSTR thus can realize more accurate semantic-guided and structure-preserved texture transfer. Note that the matching and reassembling steps actually only add two convolutional layers to the feed-forward networks, and thus their implementation is very efficient.

**Statistics-based Enhancement (SE).** This operation aims to enhance the holistic effects of the stylized target image based on global statistics matching. Either the first-order statistics (e.g., mean and standard deviation) (Huang and Belongie 2017) or the second-order statistics (e.g., covariance) (Li et al. 2017) can be adopted. In practice, we find the first-order statistics can work better in our task. As shown in the last column of Fig. 4, though higher-order statistics can reproduce the surface gloss of ceramic teapot more faithfully, they may produce inferior results with hazy shadows and consume much more time. Thus, we define our SE operation as a simple first-order statistics matching.

$$SE(F^{S_{sty}}, F^{T_{sty}}) = \sigma(F^{S_{sty}}) \left( \frac{F^{T_{sty}} - \mu(F^{T_{sty}})}{\sigma(F^{T_{sty}})} \right) + \mu(F^{S_{sty}}), \quad (5)$$

where  $\mu$  and  $\sigma$  are the mean and standard deviation.

### 3.2 Global View Structure Alignment Stage

As introduced in Sec. 3.1, the goal of this stage is to preserve the inner structures of the source textures as completely as possible so as to provide good structure guidance for subsequent stages. An important intuition we will use is that the inner structures with different scales can be captured from different views, and if we process from the global view, then the complete inner structures can be captured. For example, as we plotted in the semantic maps of Fig. 3, if we match  $T_{sem}$  and  $S_{sem}$  from a local view (i.e., use a small patch size  $p$ ), only the patches covering small or boundary structures in  $T_{sem}$  (e.g., patch  $a_1$  and  $b_1$ ) can find the proper counterparts in  $S_{sem}$  (patch  $a_2$  and  $b_2$ ). For those in the large plain regions (e.g., patch  $c_1$ ), it is hard to choose their best-suited partners among internal source patches (e.g., patch  $c_2$  and  $c_3$ ), since they are completely identical (both full-blue). Thus, the inner structures in these regions cannot be retained, and the results would show severe wash-out effects, like image (b) in the right part of Fig. 3 (where only the local view of stage II (Sec. 3.3) is used). However, if we enlarge the view of these hard patches to include some salient structures (e.g., patch  $d_1$ ), they can easily find the proper counterparts in  $S_{sem}$  again (patch  $d_2$ ). At this point, the complete inner structures can be well captured and preserved.

Following this intuition, we make a global view setting in the VSTR of this stage to handle the feature maps from the global view, i.e., using a dynamic global/maximum patch size  $p$  to cover the inner structures as completely as possible:

$$p = \min[H(F^S), W(F^S), H(F^T), W(F^T)] - 1, \quad (6)$$

where  $H$  and  $W$  denote the height and width of the features. Unfortunately, operating directly on these large patches will severely grow the computation and time cost. To alleviate this issue, we resort to the deepest layer (i.e., *Relu5\_1*) of

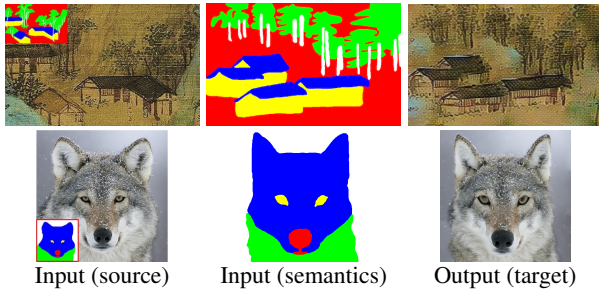


Figure 5: Doodles-to-artworks.

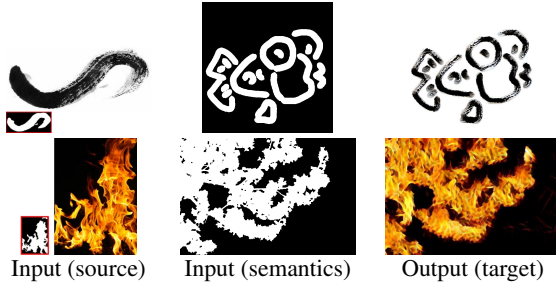


Figure 6: Texture Pattern Editing.

VGG-19 to implement the global alignment, which kills two birds with one stone: (1) The costs can be minimized, since the features at this layer have the smallest size (see the efficiency comparison below  $T_{sty}$  and image (a) in Fig. 3). (2) This layer provides the highest-level structure features and the largest receptive field, perfectly suitable for this stage. For validation, we use a small local view (*i.e.*,  $p = 3$ ) in this stage to obtain the right image (a) of Fig. 3. As observed in the red rectangle area, the result still suffers from wash-out effects that lose the inner structures, but here the effects are alleviated to some extent compared to the right image (b) (which is aligned at a shallower layer  $Relu4_1$ ). It indicates that our global view setting can help capture more intact inner structures, and the deeper VGG layer can provide higher-level structure features and larger receptive fields for better global alignment.

### 3.3 Local View Texture Refinement Stage

This stage takes the output of stage I as the input temporary stylized target image  $T_{sty}^t$  to guide a more detailed synthesis. Similar to stage I, it also uses VSTR to process the bottleneck features. The difference is, we process the features at a relatively shallower layer  $Relu4_1$ , and use a much smaller patch size (*i.e.*,  $p = 3$ ) to handle the features from only the local view. The effect of this stage can be inferred by comparing  $T_{sty}$  with the right image (c) in Fig. 3. The local view helps rectify and refine the local structures and texture details to a large extent, thus achieving more accurate alignment and higher quality.

### 3.4 Holistic Effect Enhancement Stage

The former two stages have been able to transfer satisfying inner structures and texture details. However, as they are based on high-level features, the synthesized images often neglect the low-level holistic effects (*e.g.*, colors, brightness, and contrast), as shown in the right image (d) of Fig. 3. To

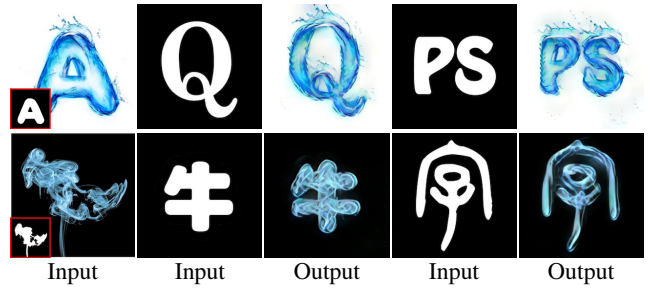


Figure 7: Text Effects Transfer.



Figure 8: Virtual Clothing Manipulation.

further enhance these low-level effects, this stage utilizes the statistics-based enhancement (SE) on the low-level features at three shallow layers, *i.e.*,  $ReluX_1$  ( $X=1,2,3$ ). As such, we can finally synthesize high-quality results which perform well in both high-level structures and low-level effects. Note that though our VSTR can also be used here to enhance the low-level effects, we do not recommend it as it will severely increase the time cost and memory requirement.

## 4 Experimental Results

### 4.1 Implementation Details

We adopt concatenation as the default setting to fuse semantic guidance. The hyperparameters that control the semantic-awareness (Eq. 4) in stage I and stage II are set to  $\omega_1 = \omega_2 = 50$  ( $\omega_1$  for stage I,  $\omega_2$  for stage II. See *supplementary material (SM)* for their effects).

### 4.2 Applications

Our framework can be effectively applied to multiple interactive texture transfer tasks, such as doodles-to-artworks, texture pattern editing, text effects transfer, and virtual clothing manipulation (see the examples in Fig. 1, 5, 6, 7, 8).

**Doodles-to-artworks.** This task aims to turn the two-bit doodles annotated by users into fine artworks with similar styles as the given exemplar paintings or photographs. Some of our results are shown in Fig. 5. See more in *SM*.

**Texture Pattern Editing.** As illustrated in Fig. 6, given an exemplar image, users can edit the texture patterns such as path and shape according to their needs. This provides a controllable way to modify the existing patterns.

**Text Effects Transfer.** As shown in Fig. 7, our method is also effective for text effects transfer which can migrate the

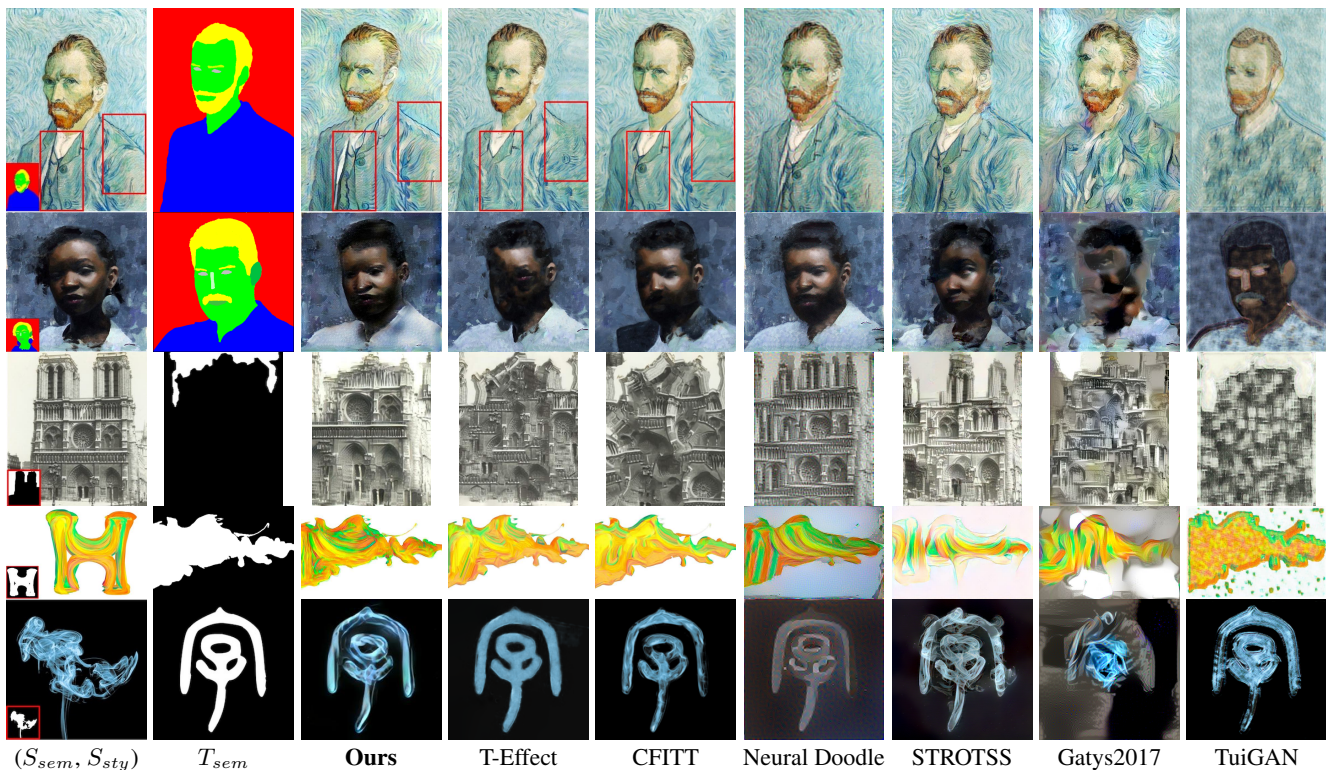


Figure 9: Qualitative comparison with the state-of-the-art universal interactive texture transfer methods. See more in *SM*.

artistic effects of stylized text images or source styles onto arbitrary raw plain texts.

**Virtual Clothing Manipulation.** Manipulating the clothing textures and distributions in a virtual way is an interesting and practical problem that has attracted much attention in recent years (Han et al. 2018, 2019a,b). Existing methods customized for this task usually learn the generation from a large-scale dataset (Liu et al. 2016). Unlike them, our framework can also be applied to this task, but it generates the result using only one exemplar image. As shown in Fig. 8, our method can transfer the clothing or painting textures to other clothing (*e.g.*, (a) and (b)), virtually try on target clothing (*e.g.*, (c)), or edit the clothing shape (*e.g.*, (d)).

### 4.3 Comparisons

We compare our method with SOTA universal interactive texture transfer algorithms including two conventional methods (T-Effect (Yang et al. 2017) and CFITT (Men et al. 2018)), three neural-based methods (Neural Doodle (Champanand 2016), STROTSS (Kolkin, Salavon, and Shakhnarovich 2019), and Gatys2017 (Gatys et al. 2017)), and one GAN-based method (TuiGAN (Lin et al. 2020)). For a fair comparison, we use their default settings except that the content weights of Neural Doodle, STROTSS, and Gatys2017 are set to 0, as there is no content image corresponding to  $T_{sem}$  in our task.

**Qualitative Comparison.** The qualitative results are shown in Fig. 9. Compared with T-Effect and CFITT, our method can synthesize higher quality results with better-preserved structures (*e.g.*, the red rectangle areas in the 1<sup>st</sup>

Table 1: Quantitative Comparison.  $\uparrow$ : Higher is better.  $\downarrow$ : Lower is better.

Method	SSIM $\uparrow$	LPIPS $\downarrow$	Style Loss $\downarrow$
T-Effect	0.276	0.449	0.740
CFITT	0.343	0.466	0.746
Neural Doodle	0.302	0.481	0.867
STROTSS	0.315	0.423	0.738
Gatys2017	0.200	0.578	0.639
TuiGAN	0.247	0.654	1.195
Ours	<b>0.372</b>	<b>0.384</b>	<b>0.497</b>

row, the face or clothing areas in the 2<sup>nd</sup> row, and the building structures in the 3<sup>rd</sup> row) and more vivid stylization effects (*e.g.*, the bottom two rows). For Neural Doodle, as it only bases on high-level features, it fails to reproduce clear images with low-level details and often introduces pixel noises. Moreover, STROTSS cannot achieve accurate semantic guidance, producing poor results with missing details (*e.g.*, the eyes in the 1<sup>st</sup> row) and misaligned structures (*e.g.*, the 2<sup>nd</sup> and 3<sup>rd</sup> rows). Gatys2017 matches the global statistics (*i.e.*, Gram matrix) for each semantic area, which cannot preserve the local texture structures. TuiGAN is hard to learn the underlying relationship between two images with a large domain gap (*e.g.*, semantic map and painting), thus cannot translate the exquisite texture details appropriately.

**Quantitative Comparison.** In addition to the visual comparison, we also make a quantitative comparison. We adopt the Structural Similarity Index (SSIM) (Wang et al. 2004) and the Learned Perceptual Image Patch Similarity

Table 2: Execution time comparison. OOM: out of memory.

Method <sup>1</sup>	256 × 256 (sec)		512 × 512 (sec)	
	CPU	GPU	CPU	GPU
T-Effect	101.52	-	241.85	-
CFITT	112.05	-	572.21	-
Neural Doodle	$\sim 2.8 \times 10^3$	178.78	$\sim 1.6 \times 10^4$	$\sim 1.1 \times 10^3$
STROTSS	$\sim 1.4 \times 10^3$	262.32	$\sim 3.9 \times 10^3$	668.84
Gatys2017	$\sim 2.2 \times 10^3$	144.78	$\sim 1.0 \times 10^4$	574.81
TuiGAN	-	$\sim 1.8 \times 10^4$	-	OOM
Ours	<b>2.573</b>	<b>0.232</b>	<b>12.381</b>	<b>0.956</b>

<sup>1</sup> Tested on a 3.3 GHz hexa-core CPU and a 6GB Nvidia 1060 GPU.

(LPIPS) (Zhang et al. 2018) between the stylized source images and the synthesized stylized target images as the metrics to measure the performance of the structure information preservation in texture transfer. Inspired by (Gatys, Ecker, and Bethge 2016; Huang and Belongie 2017), we also use the style loss between the stylized source images and the synthesized stylized target images to assess the ability to transfer the holistic styles of the stylized source images. As Table 1 shows, our method achieves the highest SSIM score and the lowest LPIPS score and style loss, which indicates that the proposed method not only has a stronger ability to preserve more structure information of the stylized source textures, but also can better transfer the holistic styles of the stylized source images.

**Efficiency.** In Table 2, we compare the running time with the competitors. Compared with conventional methods T-Effect and CFITT on CPU, our method achieves 1-2 orders of magnitude faster in resolution  $256 \times 256$  and  $512 \times 512$ . Our speed can be further accelerated by using a GPU card, eventually reaching 2-5 orders of magnitude faster than SOTA. Note that TuiGAN needs several hours and much more memory to train a model for each image pair.

**User Study.** We also conduct a user study to evaluate the quality quantitatively. Given unlimited time, 50 users are asked to select the favorite ones from 40 octets of images comprising three inputs ( $S_{sty}$ ,  $S_{sem}$ ,  $T_{sem}$ ), and five randomly shuffled outputs (T-Effect, CFITT, Neural Doodle, STROTSS, and ours<sup>1</sup>). We collect 2000 responses in total. The statistics indicate that our method achieves subjectively preferred results (**32.1%**) than T-Effect (23.8%), CFITT (26.2%), Neural Doodle (10.3%), and STROTSS (7.6%).

## 5 Discussion and Conclusion

In this paper, we propose a novel neural-based framework, dubbed *texture reformer*, for fast and universal interactive texture transfer. A feed-forward multi-view and multi-stage synthesis procedure is imposed to synthesize high-quality results with coherent structures and fine texture details from coarse to fine. Moreover, we also introduce a novel learning-free *view-specific texture reformation (VSTR)* operation with a new semantic map guidance strategy to realize more accurate semantic-guided and structure-preserved texture transfer. Experimental results demonstrate the effectiveness of

<sup>1</sup>Gatys2017 and TuiGAN are not compared here because the quality of their results is clearly inferior to ours, as shown in Fig. 9.

our framework on many texture transfer tasks. And compared with SOTA algorithms, it not only achieves higher quality results but also is 2-5 orders of magnitude faster.

However, the method still suffers from some limitations. The inherent nature of patch alignment used in the VSTR operation may result in a few quality issues. And since our framework does not make patches rotated or scaled, it may not work very well for semantic maps with drastically different shapes and large geometric deformation. Besides, since our method does not use any additional structure guidance or distribution constraint, it may fail to achieve correct texture transfer for patterns with decorative elements. We strongly encourage the readers to refer to the *SM* for the comprehensive discussions on our limitations.

There are also a lot of prior arts that can give enlightenment to improve our method. For example, one may consider integrating the histogram matching techniques in (Risser, Wilmot, and Barnes 2017) into our VSTR or SE operations to improve the performance. To preserve the shading of the source textures, one may consider adding the lighting map constraint like (Tsin, Liu, and Ramesh 2001) on the intermediate features of our VSTR or SE operations. To achieve geometric texture transfer, one may model a deformation field like (Liu, Lin, and Hays 2004), or borrow some ideas from recent geometric style transfer approaches (Kim et al. 2020; Liu, Yang, and Hall 2021). Given the simplicity of our framework, we believe there is substantial room for improvement. In addition, the compression and acceleration of the framework to achieve real-time interactive texture transfer is also a practical direction worthy of further exploration.

## Acknowledgements

This work was supported in part by the projects No. 2020YFC1523101, 19ZDA197, LY21F020005, 2021009, 2019C03137, NSFC project: research on key technologies of art image restoration based on decoupling learning (62172365), MOE Frontier Science Center for Brain Science & Brain-Machine Integration (Zhejiang University), and Key Scientific Research Base for Digital Conservation of Cave Temples (Zhejiang University), State Administration for Cultural Heritage.

## References

- An, J.; Huang, S.; Song, Y.; Dou, D.; Liu, W.; and Luo, J. 2021. ArtFlow: Unbiased Image Style Transfer via Reversible Neural Flows. In *Proceedings of the IEEE Conference on Computer Vision and Pattern Recognition (CVPR)*, 862–871.
- Barnes, C.; Shechtman, E.; Finkelstein, A.; and Goldman, D. B. 2009. PatchMatch: A randomized correspondence algorithm for structural image editing. *ACM Transactions on Graphics (TOG)*, 28(3): 24.
- Barnes, C.; Shechtman, E.; Goldman, D. B.; and Finkelstein, A. 2010. The generalized patchmatch correspondence algorithm. In *Proceedings of the European Conference on Computer Vision (ECCV)*, 29–43. Springer.
- Bookstein, F. L. 1989. Principal warps: Thin-plate splines and the decomposition of deformations. *IEEE Transactions on Pattern Analysis and Machine Intelligence (TPAMI)*, 11(6): 567–585.



- Champanand, A. J. 2016. Semantic style transfer and turning two-bit doodles into fine artworks. *arXiv preprint arXiv:1603.01768*.
- Chen, H.; Zhao, L.; Qiu, L.; Wang, Z.; Zhang, H.; Xing, W.; and Lu, D. 2020. Creative and diverse artwork generation using adversarial networks. *IET Computer Vision*, 14(8): 650–657.
- Chen, H.; Zhao, L.; Wang, Z.; Ming, Z. H.; Zuo, Z.; Li, A.; Xing, W.; and Lu, D. 2021a. Artistic Style Transfer with Internal-external Learning and Contrastive Learning. In *Thirty-Fifth Conference on Neural Information Processing Systems (NeurIPS)*.
- Chen, H.; Zhao, L.; Wang, Z.; Zhang, H.; Zuo, Z.; Li, A.; Xing, W.; and Lu, D. 2021b. DualAST: Dual Style-Learning Networks for Artistic Style Transfer. In *Proceedings of the IEEE Conference on Computer Vision and Pattern Recognition (CVPR)*, 872–881.
- Chen, H.; Zhao, L.; Zhang, H.; Wang, Z.; Zuo, Z.; Li, A.; Xing, W.; and Lu, D. 2021c. Diverse image style transfer via invertible cross-space mapping. In *Proceedings of the IEEE/CVF International Conference on Computer Vision (ICCV)*, 14880–14889.
- Chen, T. Q.; and Schmidt, M. 2016. Fast patch-based style transfer of arbitrary style. *arXiv preprint arXiv:1612.04337*.
- Chen, W.; and Hays, J. 2018. Sketchygan: Towards diverse and realistic sketch to image synthesis. In *Proceedings of the IEEE Conference on Computer Vision and Pattern Recognition (CVPR)*, 9416–9425.
- Cheng, J.; Jaiswal, A.; Wu, Y.; Natarajan, P.; and Natarajan, P. 2021. Style-Aware Normalized Loss for Improving Arbitrary Style Transfer. In *Proceedings of the IEEE Conference on Computer Vision and Pattern Recognition (CVPR)*, 134–143.
- Darabi, S.; Shechtman, E.; Barnes, C.; Goldman, D. B.; and Sen, P. 2012. Image melding: Combining inconsistent images using patch-based synthesis. *ACM Transactions on graphics (TOG)*, 31(4): 1–10.
- Efros, A. A.; and Freeman, W. T. 2001. Image quilting for texture synthesis and transfer. In *Proceedings of the 28th annual conference on Computer graphics and interactive techniques*, 341–346.
- Efros, A. A.; and Leung, T. K. 1999. Texture synthesis by non-parametric sampling. In *Proceedings of the IEEE International Conference on Computer Vision (ICCV)*, 1033. IEEE.
- Frigo, O.; Sabater, N.; Delon, J.; and Hellier, P. 2016. Split and match: Example-based adaptive patch sampling for unsupervised style transfer. In *Proceedings of the IEEE Conference on Computer Vision and Pattern Recognition (CVPR)*, 553–561.
- Frühstück, A.; Alhashim, I.; and Wonka, P. 2019. Tilegan: synthesis of large-scale non-homogeneous textures. *ACM Transactions on Graphics (TOG)*, 38(4): 1–11.
- Gatys, L.; Ecker, A. S.; and Bethge, M. 2015. Texture synthesis using convolutional neural networks. In *Advances in Neural Information Processing Systems (NeurIPS)*, 262–270.
- Gatys, L. A.; Ecker, A. S.; and Bethge, M. 2016. Image style transfer using convolutional neural networks. In *Proceedings of the IEEE Conference on Computer Vision and Pattern Recognition (CVPR)*, 2414–2423.
- Gatys, L. A.; Ecker, A. S.; Bethge, M.; Hertzmann, A.; and Shechtman, E. 2017. Controlling perceptual factors in neural style transfer. In *Proceedings of the IEEE Conference on Computer Vision and Pattern Recognition (CVPR)*, 3985–3993.
- Goferman, S.; Zelnik-Manor, L.; and Tal, A. 2011. Context-aware saliency detection. *IEEE Transactions on Pattern Analysis and Machine Intelligence (TPAMI)*, 34(10): 1915–1926.
- Goodfellow, I.; Pouget-Abadie, J.; Mirza, M.; Xu, B.; Warde-Farley, D.; Ozair, S.; Courville, A.; and Bengio, Y. 2014. Generative adversarial nets. In *Advances in Neural Information Processing Systems (NeurIPS)*, 2672–2680.
- Gu, S.; Chen, C.; Liao, J.; and Yuan, L. 2018. Arbitrary Style Transfer with Deep Feature Reshuffle. In *Proceedings of the IEEE Conference on Computer Vision and Pattern Recognition (CVPR)*, 8222–8231.
- Haeberli, P. 1990. Paint by numbers: Abstract image representations. In *Proceedings of the 17th annual conference on Computer graphics and interactive techniques*, 207–214.
- Han, X.; Hu, X.; Huang, W.; and Scott, M. R. 2019a. Clothflow: A flow-based model for clothed person generation. In *Proceedings of the IEEE International Conference on Computer Vision (ICCV)*, 10471–10480.
- Han, X.; Wu, Z.; Huang, W.; Scott, M. R.; and Davis, L. S. 2019b. Finet: Compatible and diverse fashion image inpainting. In *Proceedings of the IEEE International Conference on Computer Vision (ICCV)*, 4481–4491.
- Han, X.; Wu, Z.; Wu, Z.; Yu, R.; and Davis, L. S. 2018. Viton: An image-based virtual try-on network. In *Proceedings of the IEEE Conference on Computer Vision and Pattern Recognition (CVPR)*, 7543–7552.
- Hertzmann, A.; Jacobs, C. E.; Oliver, N.; Curless, B.; and Salesin, D. H. 2001. Image analogies. In *Proceedings of the 28th annual conference on Computer graphics and interactive techniques*, 327–340.
- Huang, X.; and Belongie, S. 2017. Arbitrary style transfer in real-time with adaptive instance normalization. In *Proceedings of the IEEE International Conference on Computer Vision (ICCV)*, 1501–1510.
- Isola, P.; Zhu, J.-Y.; Zhou, T.; and Efros, A. A. 2017. Image-to-image translation with conditional adversarial networks. In *Proceedings of the IEEE Conference on Computer Vision and Pattern Recognition (CVPR)*, 1125–1134.
- Jing, Y.; Liu, X.; Ding, Y.; Wang, X.; Ding, E.; Song, M.; and Wen, S. 2020. Dynamic instance normalization for arbitrary style transfer. In *Proceedings of the AAAI Conference on Artificial Intelligence (AAAI)*, volume 34, 4369–4376.
- Jing, Y.; Liu, Y.; Yang, Y.; Feng, Z.; Yu, Y.; Tao, D.; and Song, M. 2018. Stroke controllable fast style transfer with adaptive receptive fields. In *Proceedings of the European Conference on Computer Vision (ECCV)*, 238–254.
- Johnson, J.; Alahi, A.; and Fei-Fei, L. 2016. Perceptual losses for real-time style transfer and super-resolution. In *Proceedings of the European Conference on Computer Vision (ECCV)*, 694–711. Springer.
- Kim, S. S.; Kolkin, N.; Salavon, J.; and Shakhnarovich, G. 2020. Deformable style transfer. In *Proceedings of the European Conference on Computer Vision (ECCV)*, 246–261. Springer.
- Kolkin, N.; Salavon, J.; and Shakhnarovich, G. 2019. Style Transfer by Relaxed Optimal Transport and Self-Similarity. In *Proceedings of the IEEE Conference on Computer Vision and Pattern Recognition (CVPR)*, 10051–10060.
- Kwatra, V.; Essa, I.; Bobick, A.; and Kwatra, N. 2005. Texture optimization for example-based synthesis. *ACM Transactions on Graphics (TOG)*, 24(3): 795–802.
- Li, C.; and Wand, M. 2016a. Combining markov random fields and convolutional neural networks for image synthesis. In *Proceedings of the IEEE Conference on Computer Vision and Pattern Recognition (CVPR)*, 2479–2486.
- Li, C.; and Wand, M. 2016b. Precomputed real-time texture synthesis with markovian generative adversarial networks. In *Proceedings of the European Conference on Computer Vision (ECCV)*, 702–716. Springer.

- Li, Y.; Fang, C.; Yang, J.; Wang, Z.; Lu, X.; and Yang, M.-H. 2017. Universal style transfer via feature transforms. In *Advances in Neural Information Processing Systems (NeurIPS)*, 386–396.
- Liao, J.; Yao, Y.; Yuan, L.; Hua, G.; and Kang, S. B. 2017. Visual attribute transfer through deep image analogy. *ACM Transactions on Graphics (TOG)*.
- Lin, J.; Pang, Y.; Xia, Y.; Chen, Z.; and Luo, J. 2020. TuiGAN: Learning Versatile Image-to-Image Translation with Two Unpaired Images. In *Proceedings of the European Conference on Computer Vision (ECCV)*.
- Lin, T.; Ma, Z.; Li, F.; He, D.; Li, X.; Ding, E.; Wang, N.; Li, J.; and Gao, X. 2021. Drafting and Revision: Laplacian Pyramid Network for Fast High-Quality Artistic Style Transfer. In *Proceedings of the IEEE Conference on Computer Vision and Pattern Recognition (CVPR)*, 5141–5150.
- Lin, T.-Y.; Maire, M.; Belongie, S.; Hays, J.; Perona, P.; Ramanan, D.; Dollár, P.; and Zitnick, C. L. 2014. Microsoft coco: Common objects in context. In *Proceedings of the European Conference on Computer Vision (ECCV)*, 740–755. Springer.
- Liu, X.-C.; Yang, Y.-L.; and Hall, P. 2021. Learning To Warp for Style Transfer. In *Proceedings of the IEEE/CVF Conference on Computer Vision and Pattern Recognition (CVPR)*, 3702–3711.
- Liu, Y.; Lin, W.-C.; and Hays, J. 2004. Near-regular texture analysis and manipulation. *ACM Transactions on Graphics (TOG)*, 23(3): 368–376.
- Liu, Z.; Luo, P.; Qiu, S.; Wang, X.; and Tang, X. 2016. Deepfashion: Powering robust clothes recognition and retrieval with rich annotations. In *Proceedings of the IEEE Conference on Computer Vision and Pattern Recognition (CVPR)*, 1096–1104.
- Lu, J.; Barnes, C.; DiVerdi, S.; and Finkelstein, A. 2013. Real-Brush: painting with examples of physical media. *ACM Transactions on Graphics (TOG)*, 32(4): 1–12.
- Lu, J.; Barnes, C.; Wan, C.; Asente, P.; Mech, R.; and Finkelstein, A. 2014. DecoBrush: drawing structured decorative patterns by example. *ACM Transactions on Graphics (TOG)*, 33(4): 1–9.
- Lu, J.; Yu, F.; Finkelstein, A.; and DiVerdi, S. 2012. HelpingHand: Example-based stroke stylization. *ACM Transactions on Graphics (TOG)*, 31(4): 1–10.
- Lu, M.; Zhao, H.; Yao, A.; Chen, Y.; Xu, F.; and Zhang, L. 2019. A Closed-Form Solution to Universal Style Transfer. In *Proceedings of the IEEE International Conference on Computer Vision (ICCV)*, 5952–5961.
- Lu, M.; Zhao, H.; Yao, A.; Xu, F.; Chen, Y.; and Zhang, L. 2017. Decoder network over lightweight reconstructed feature for fast semantic style transfer. In *Proceedings of the IEEE International Conference on Computer Vision (ICCV)*, 2469–2477.
- Luan, F.; Paris, S.; Shechtman, E.; and Bala, K. 2017. Deep photo style transfer. In *Proceedings of the IEEE Conference on Computer Vision and Pattern Recognition (CVPR)*, 4990–4998.
- Men, Y.; Lian, Z.; Tang, Y.; and Xiao, J. 2018. A common framework for interactive texture transfer. In *Proceedings of the IEEE Conference on Computer Vision and Pattern Recognition (CVPR)*, 6353–6362.
- Mirza, M.; and Osindero, S. 2014. Conditional generative adversarial nets. *arXiv preprint arXiv:1411.1784*.
- Myronenko, A.; and Song, X. 2010. Point set registration: Coherent point drift. *IEEE Transactions on Pattern Analysis and Machine Intelligence (TPAMI)*, 32(12): 2262–2275.
- Park, D. Y.; and Lee, K. H. 2019. Arbitrary style transfer with style-attentional networks. In *Proceedings of the IEEE Conference on Computer Vision and Pattern Recognition (CVPR)*, 5880–5888.
- Risser, E.; Wilmot, P.; and Barnes, C. 2017. Stable and controllable neural texture synthesis and style transfer using histogram losses. *arXiv preprint arXiv:1701.08893*.
- Shaham, T. R.; Dekel, T.; and Michaeli, T. 2019. Singan: Learning a generative model from a single natural image. In *Proceedings of the IEEE International Conference on Computer Vision (ICCV)*, 4570–4580.
- Sheng, L.; Lin, Z.; Shao, J.; and Wang, X. 2018. Avatar-Net: Multi-scale Zero-shot Style Transfer by Feature Decoration. In *Proceedings of the IEEE Conference on Computer Vision and Pattern Recognition (CVPR)*, 8242–8250.
- Simonyan, K.; and Zisserman, A. 2014. Very deep convolutional networks for large-scale image recognition. *arXiv preprint arXiv:1409.1556*.
- Tsin, Y.; Liu, Y.; and Ramesh, V. 2001. Texture replacement in real images. In *Proceedings of the 2001 IEEE Computer Society Conference on Computer Vision and Pattern Recognition (CVPR)*, volume 2, II–II. IEEE.
- Ulyanov, D.; Lebedev, V.; Vedaldi, A.; and Lempitsky, V. S. 2016. Texture Networks: Feed-forward Synthesis of Textures and Stylized Images. In *International Conference on Machine Learning (ICML)*, 1349–1357.
- Wang, Z.; Bovik, A. C.; Sheikh, H. R.; and Simoncelli, E. P. 2004. Image quality assessment: from error visibility to structural similarity. *IEEE Transactions on Image Processing (TIP)*, 13(4): 600–612.
- Wang, Z.; Zhao, L.; Chen, H.; Qiu, L.; Mo, Q.; Lin, S.; Xing, W.; and Lu, D. 2020a. Diversified Arbitrary Style Transfer via Deep Feature Perturbation. In *Proceedings of the IEEE Conference on Computer Vision and Pattern Recognition (CVPR)*, 7789–7798.
- Wang, Z.; Zhao, L.; Chen, H.; Zuo, Z.; Li, A.; Xing, W.; and Lu, D. 2021. Evaluate and improve the quality of neural style transfer. *Computer Vision and Image Understanding (CVIU)*, 207: 103203.
- Wang, Z.; Zhao, L.; Lin, S.; Mo, Q.; Zhang, H.; Xing, W.; and Lu, D. 2020b. GLStyleNet: exquisite style transfer combining global and local pyramid features. *IET Computer Vision*, 14(8): 575–586.
- Yang, S.; Liu, J.; Lian, Z.; and Guo, Z. 2017. Awesome typography: Statistics-based text effects transfer. In *Proceedings of the IEEE Conference on Computer Vision and Pattern Recognition (CVPR)*, 7464–7473.
- Yang, S.; Wang, Z.; Wang, Z.; Xu, N.; Liu, J.; and Guo, Z. 2019. Controllable artistic text style transfer via shape-matching gan. In *Proceedings of the IEEE International Conference on Computer Vision (ICCV)*, 4442–4451.
- Zhang, C.; Zhu, Y.; and Zhu, S.-C. 2019. MetaStyle: Three-Way Trade-off among Speed, Flexibility, and Quality in Neural Style Transfer. In *Proceedings of the AAAI Conference on Artificial Intelligence (AAAI)*, volume 33, 1254–1261.
- Zhang, R.; Isola, P.; Efros, A. A.; Shechtman, E.; and Wang, O. 2018. The unreasonable effectiveness of deep features as a perceptual metric. In *Proceedings of the IEEE Conference on Computer Vision and Pattern Recognition (CVPR)*, 586–595.
- Zhao, L.; Mo, Q.; Lin, S.; Wang, Z.; Zuo, Z.; Chen, H.; Xing, W.; and Lu, D. 2020. UCTGAN: Diverse Image Inpainting Based on Unsupervised Cross-Space Translation. In *Proceedings of the IEEE Conference on Computer Vision and Pattern Recognition (CVPR)*, 5741–5750.
- Zhu, J.-Y.; Krähenbühl, P.; Shechtman, E.; and Efros, A. A. 2016. Generative visual manipulation on the natural image manifold. In *Proceedings of the European Conference on Computer Vision (ECCV)*, 597–613. Springer.

## A Supplementary Material

### A.1 Effects of the semantic hyperparameters

Semantic hyperparameters  $\omega_1$  and  $\omega_2$  control the semantic-awareness in stage I and stage II, respectively. As shown in Fig. 10, when  $\omega_1$  and  $\omega_2$  decrease, the algorithm reverts to its semantically unaware version that ignores the semantic maps provided. Due to the different views used, different stages may concentrate on different perspectives to align with the semantic maps. Specifically, stage I (1<sup>st</sup> row) is more inclined to align with the semantic maps from a global perspective, e.g., adjusting the position of the portrait or rectifying some large structures in the clothing. By contrast, stage II (2<sup>nd</sup> row) can align more detailed structures, such as faces, with the semantic maps. By using stage I and stage II together (3<sup>rd</sup> row), the result can be more faithful to the semantic maps in both large structures and small details.

### A.2 Additional interactive texture transfer results

In this part, we show some additional results generated by the proposed framework in different interactive texture transfer applications: doodles-to-artworks (Fig. 11), texture pattern editing (Fig. 12), text effects transfer (Fig. 13, 14), and virtual clothing manipulation (Fig. 15, 16).

### A.3 Additional comparisons with state-of-the-art algorithms

We provide additional comparison results of our method and the state-of-the-art universal interactive texture transfer algorithms (T-Effect (Yang et al. 2017), CFITT (Men et al. 2018), Neural Doodle (Champanand 2016), STROTSS (Kolkin, Salavon, and Shakhnarovich 2019), Gatys2017 (Gatys et al. 2017), and TuiGAN (Lin et al. 2020)) in different scenarios. As shown in Fig. 17, 18, 19, 20, 21, our approach is capable of synthesizing higher quality results with better-preserved structures and more vivid stylization effects.

### A.4 Comparison results with baseline methods

The main innovation of our work lies in the fast and universal interactive texture transfer framework. Since some of its components are based on Style-Swap (Chen and Schmidt 2016), AdaIN (Huang and Belongie 2017), and WCT (Li et al. 2017), it would be helpful to compare against them to validate the superiority of our framework. The comparison results are shown in Fig. 22, and the analyses are provided in the caption.

### A.5 Limitations and discussions

In this work, since our focus is a novel fast and universal solution for interactive texture transfer, *we prioritize flexibility and efficiency over quality*. Although our results have shown improvement over existing works, and the user study has also verified our superiority against SOTA on quality, the results are imperfect, and there are still some limitations. Given the simplicity of our proposed framework, we believe there is substantial room for improvement. In Fig. 23, 24, 25, 26, we provide some typical limitations of

our method, then analyze the reasons behind them and discuss the possible solutions to address them. The further improvement of our framework we leave as future work.

### A.6 How to balance the performance of different stages?

In our implementation code (<https://github.com/EndyWon/Texture-Reformer>), we provide some interfaces to help users to balance the performance of each stage. Users can control the performance by varying the patch size, changing the stage separation, adjusting the semantic weight, or interpolating between features (like the ways applied in (Huang and Belongie 2017) and (Li et al. 2017)). There is no optimal setting that can perfectly deal with all cases. Our default setting provides a general solution that can be applied to most cases. However, since our framework is fast, modular, and learning-free, users can easily explore the optimal settings for any specific case.



Figure 10: Effects of the hyperparameters ( $\omega_1$  and  $\omega_2$ ) to control the semantic-awareness. The default values are marked in red.



Figure 11: Doodles-to-artworks transfer results. Image courtesy of (Wang et al. 2020b; Champandard 2016; Liao et al. 2017).

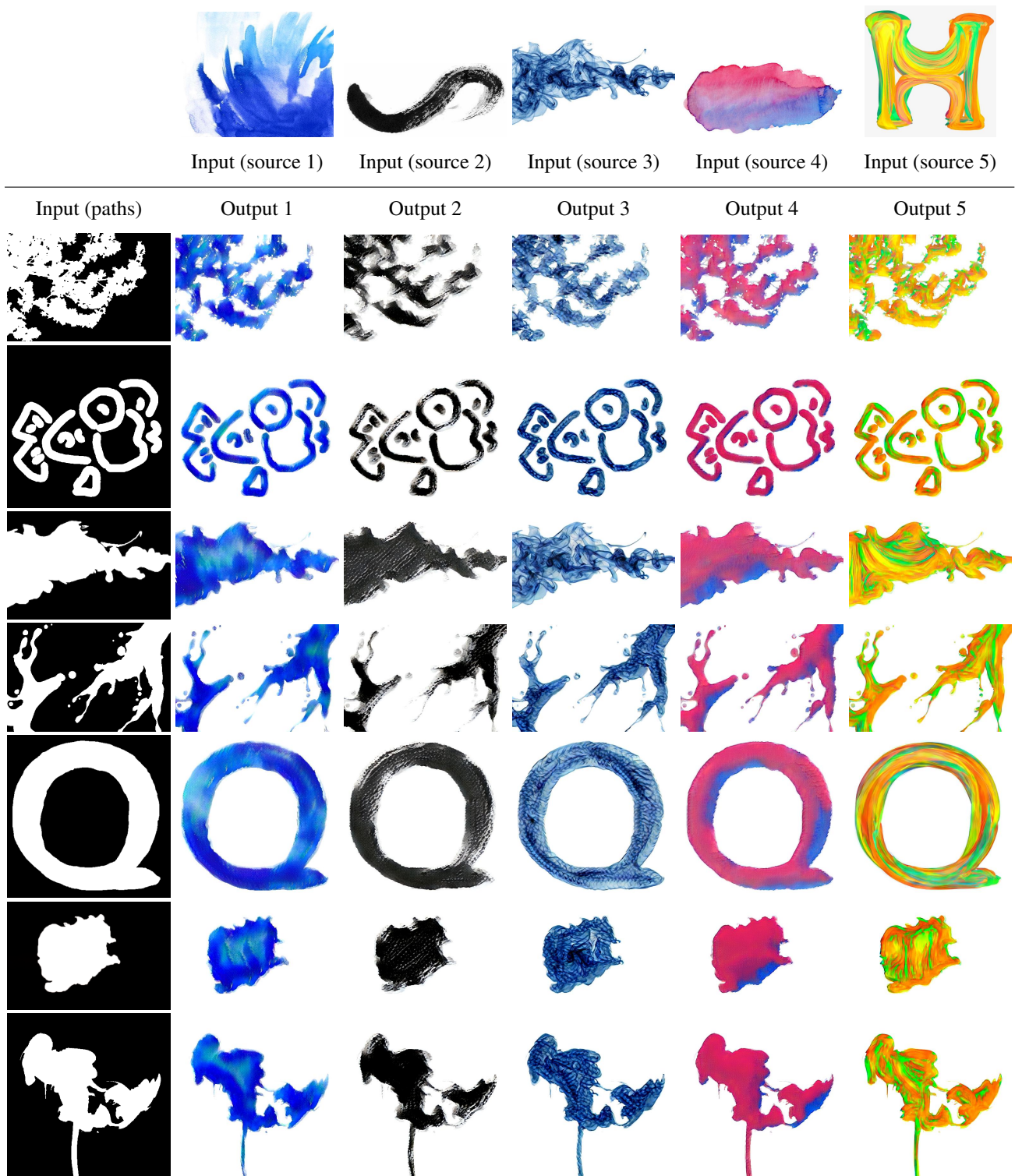


Figure 12: Texture pattern editing results. Image courtesy of (Men et al. 2018; Yang et al. 2019; Luan et al. 2017).

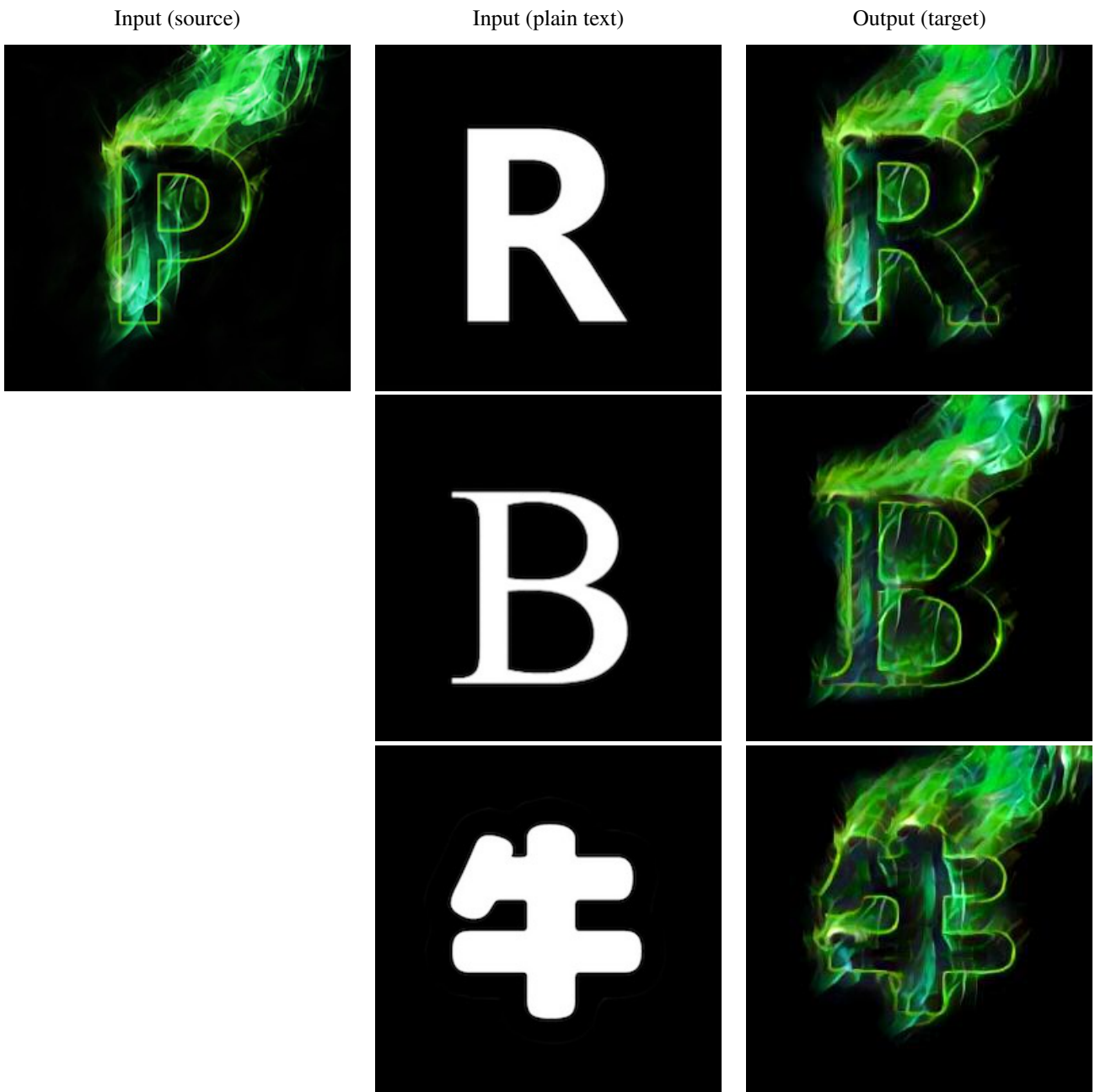


Figure 13: Text effects transfer results. Image courtesy of (Yang et al. 2017).

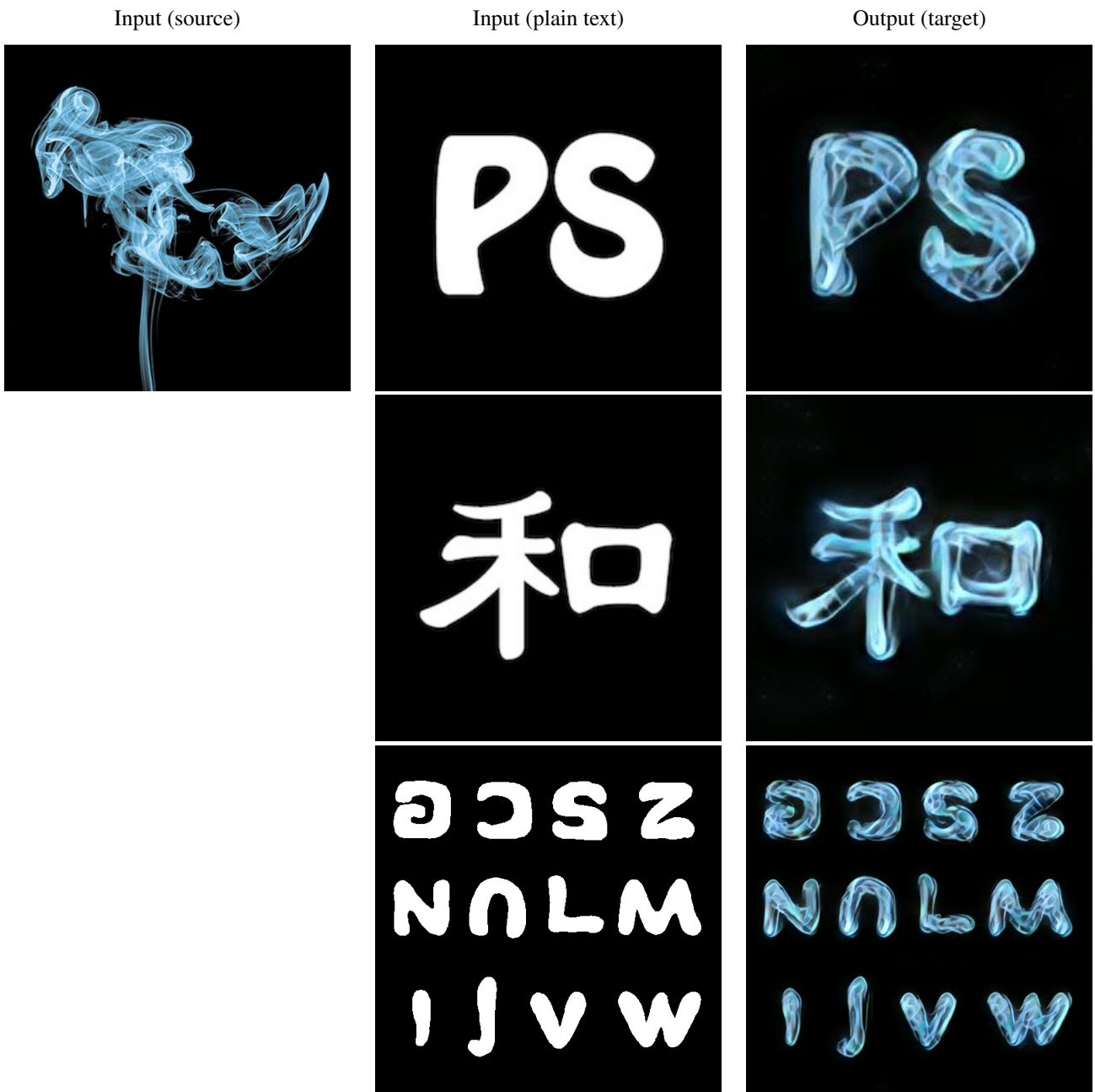


Figure 14: Text effects transfer results. Image courtesy of (Yang et al. 2017, 2019; Lu et al. 2014).





Figure 15: Virtual clothing manipulation results. Image courtesy of (Liu et al. 2016).



Input (source 1)

Input (source 2)

Input (source 3)

Input (source 4)

Input (source 5)

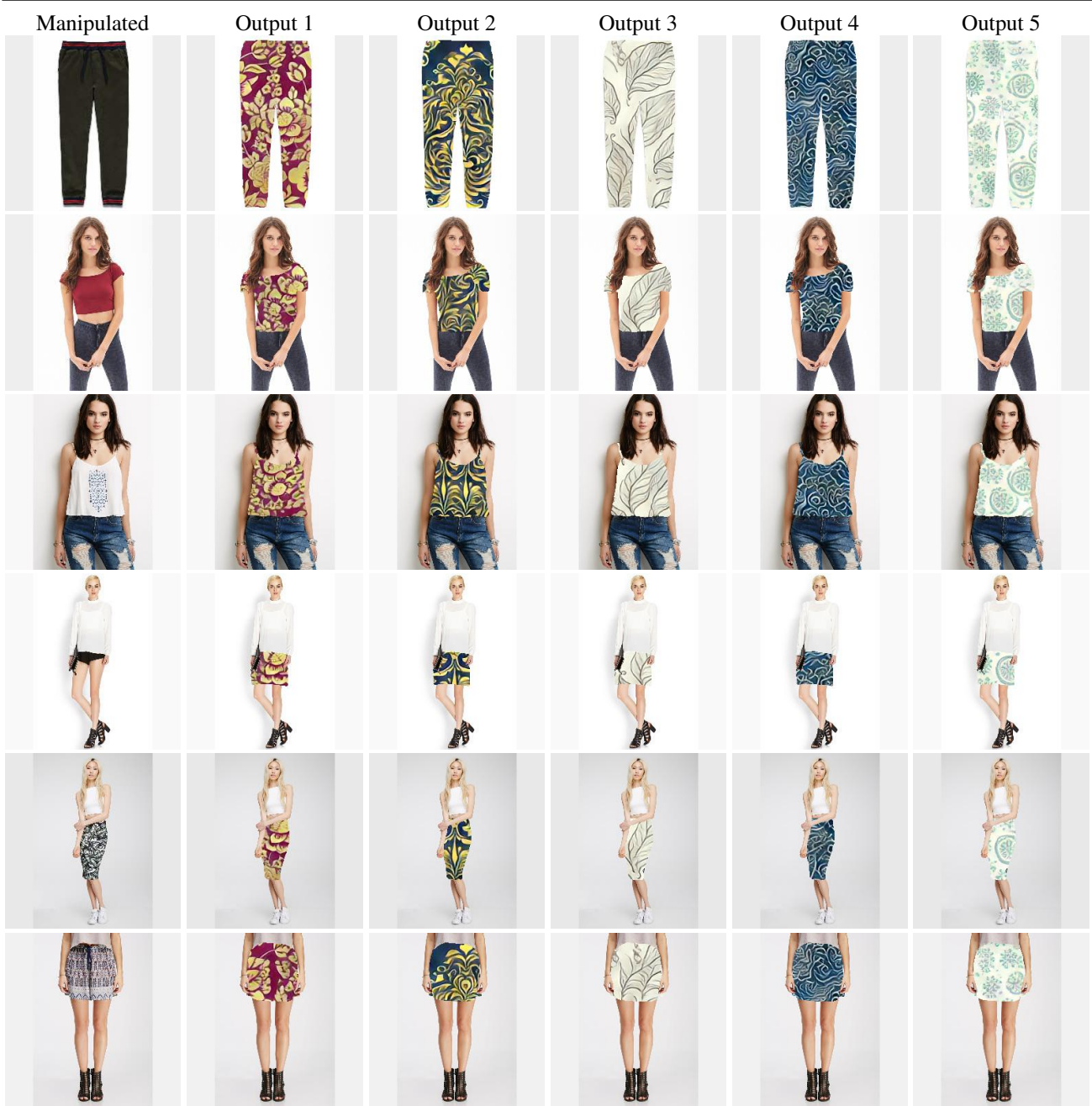
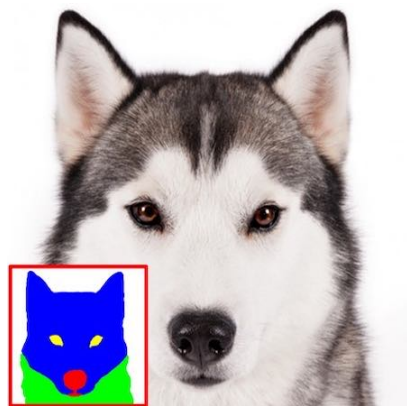


Figure 16: Virtual clothing manipulation results. Image courtesy of (Liu et al. 2016).



Source ( $S_{sty}, S_{sem}$ )



Target ( $T_{sem}$ )



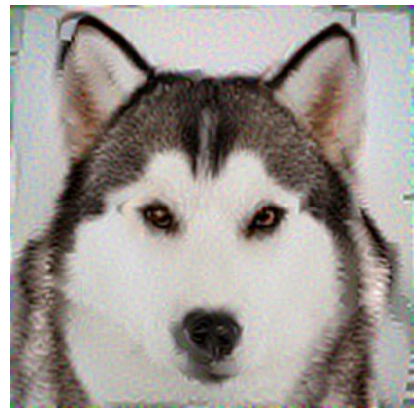
Our Method



T-Effect



CFITT



Neural Doodle



STROTSS

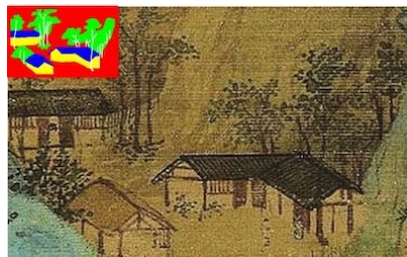


Gatys2017



TuiGAN

Figure 17: Comparison with state-of-the-art methods on the doodles-to-artworks task.



Source ( $S_{sty}, S_{sem}$ )



Target ( $T_{sem}$ )



**Our Method**



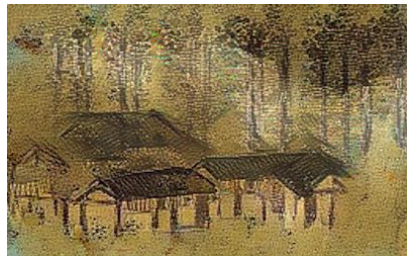
T-Effect



CFITT



Neural Doodle



STROTSS



Gatys2017



TuiGAN

Figure 18: Comparison with state-of-the-art methods on the doodles-to-artworks task.

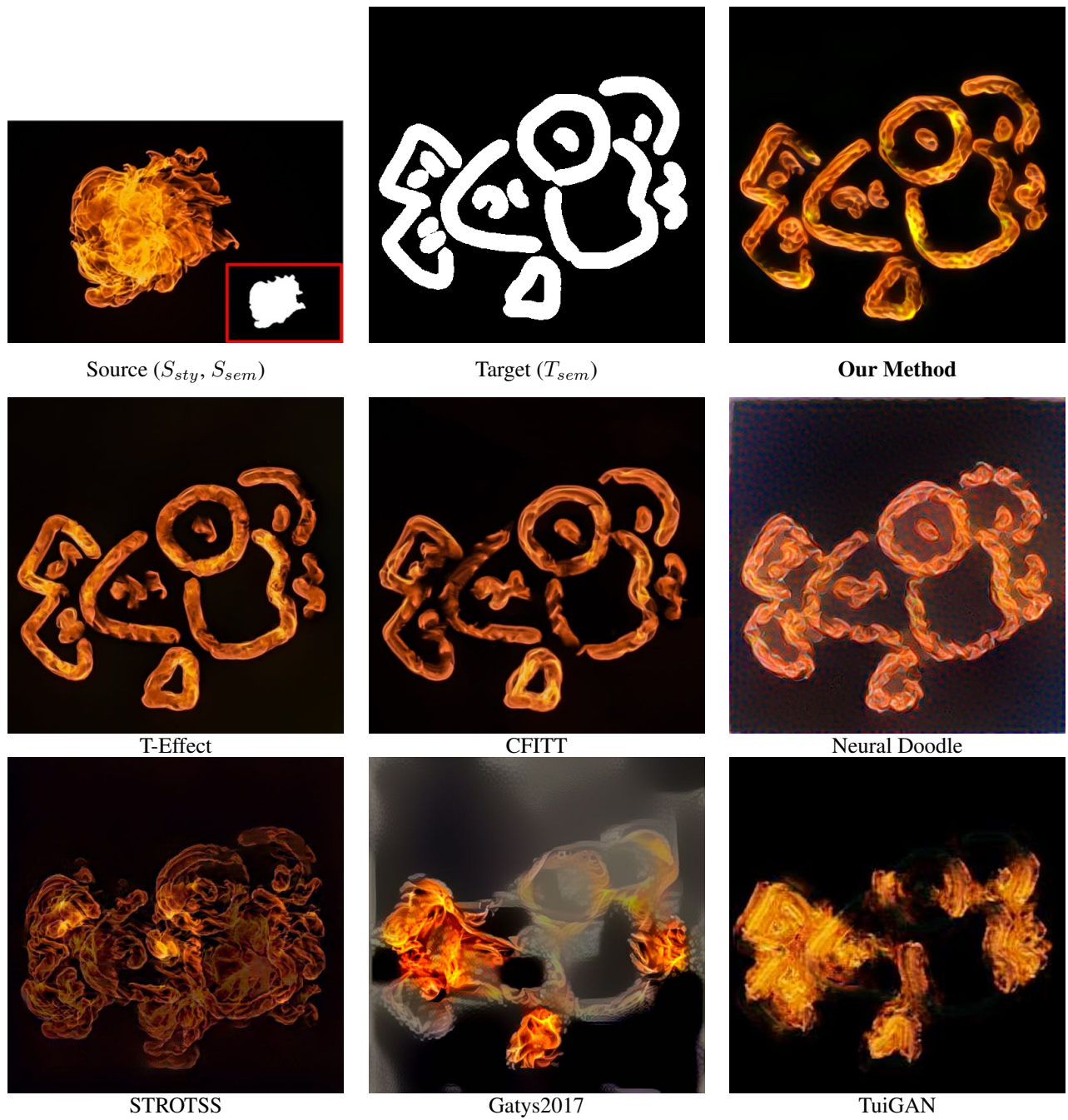


Figure 19: Comparison with state-of-the-art methods on the texture pattern editing task.

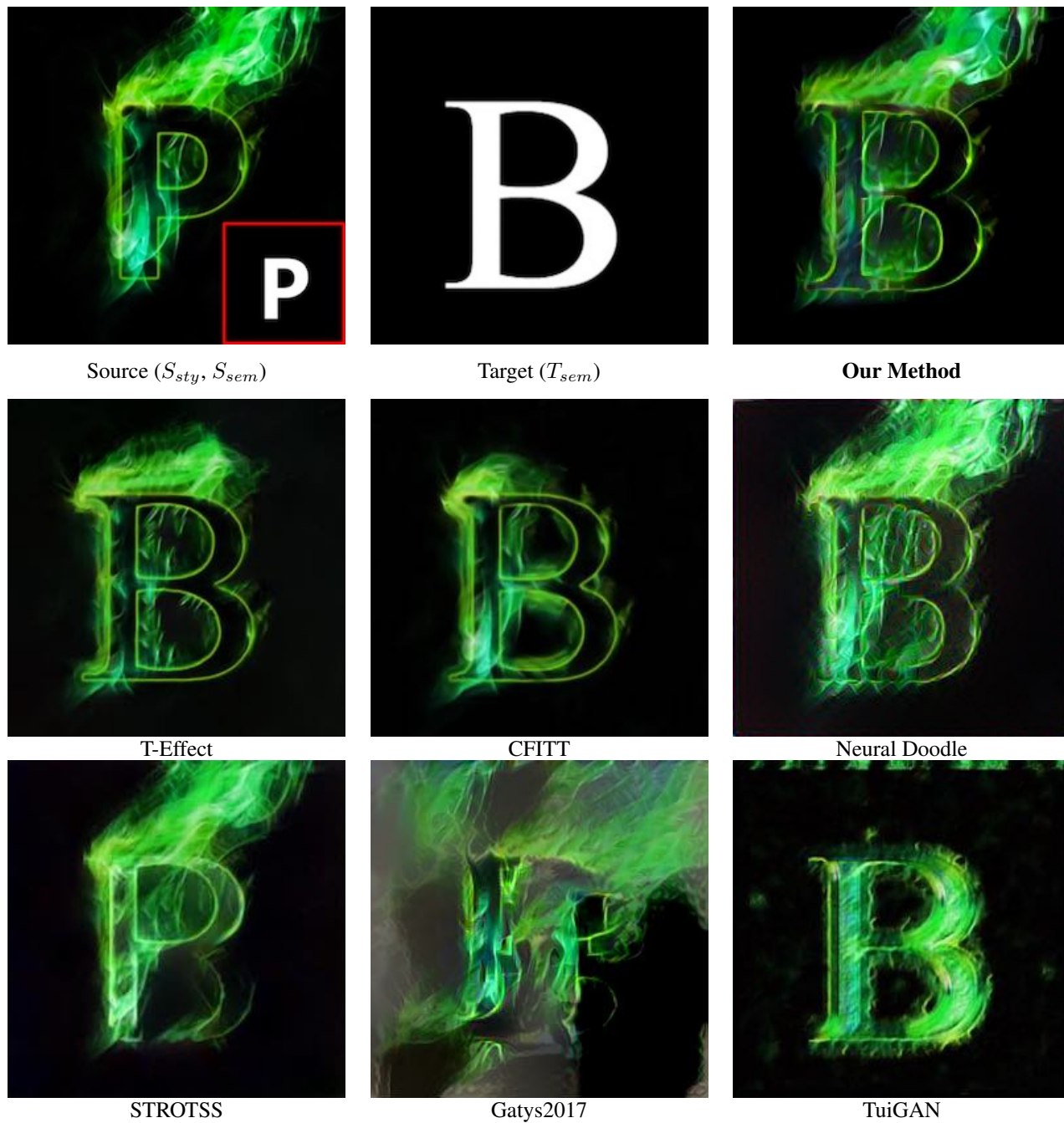


Figure 20: Comparison with state-of-the-art methods on the text effects transfer task.



Manipulated image &  $T_{sem}$



Source stylized image  $S_{sty}$



**Our Method**



T-Effect



CFITT



Neural Doodle



STROTSS



Gatys2017



TuiGAN

Figure 21: Comparison with state-of-the-art methods on the virtual clothing manipulation task.



Figure 22: Comparison results with baseline methods (Style-Swap (Chen and Schmidt 2016), AdaIN (Huang and Belongie 2017), and WCT (Li et al. 2017)). For fairness, all baselines are tailored to be interactive by introducing semantic maps. As is evident, Style-Swap and AdaIN can only produce less stylized results due to the single-level stylization (see the top row). By exploiting a multi-level mechanism, WCT and ours achieve much more vivid stylization. However, since WCT is designed to match the global statistics (i.e., covariance), it cannot transfer local textures and often introduces distorted patterns. In addition, the three baselines all fail to preserve the local texture structures (e.g., the patterns in the bottom row), while ours not only retains the complete local patterns but also transfers the vivid global texture effects, thanks to the proposed view-specific texture reformation (VSTR) operation and multi-view and multi-stage synthesis procedure (see more analyses in our main paper).



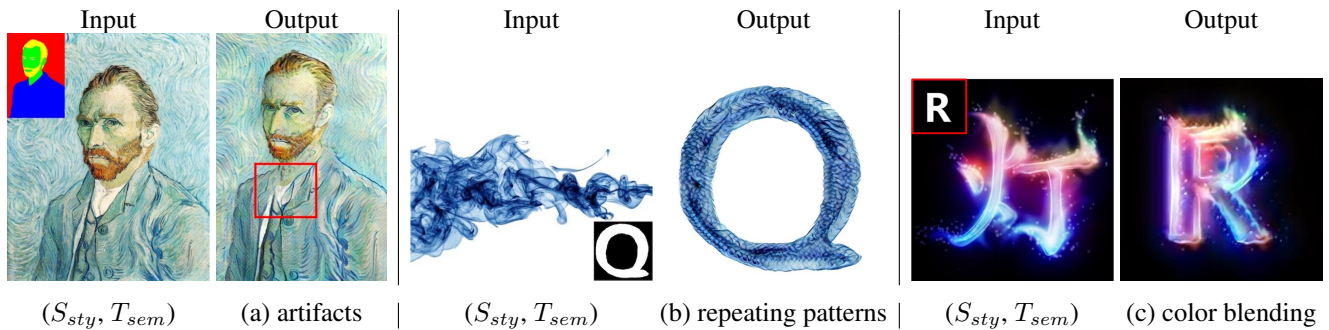


Figure 23: **Limitation of type 1: quality issues.** Some of the results generated by our method may suffer from a few quality issues, e.g., (a) noticeable artifacts, (b) smaller repeating patterns, and (c) color blending. These issues may be caused by the inherent nature of patch alignment in the VSTR we used in local refinement stage II (we removed the global alignment stage I, but these effects were not mitigated). As a well-known problem, the patch alignment is prone to introduce wash-out artifacts due to the repetitive use of the same patches (Gu et al. 2018; Sheng et al. 2018), and sometimes may cause color blending problem due to the averaging of overlapping patches (Chen and Schmidt 2016). Nevertheless, we still utilize it in our framework due to its flexibility and efficiency. The further improvement can be achieved by improving the VSTR operation, or integrating additional guidances like (Men et al. 2018), or more straightforwardly, specifying more elaborate semantic maps.

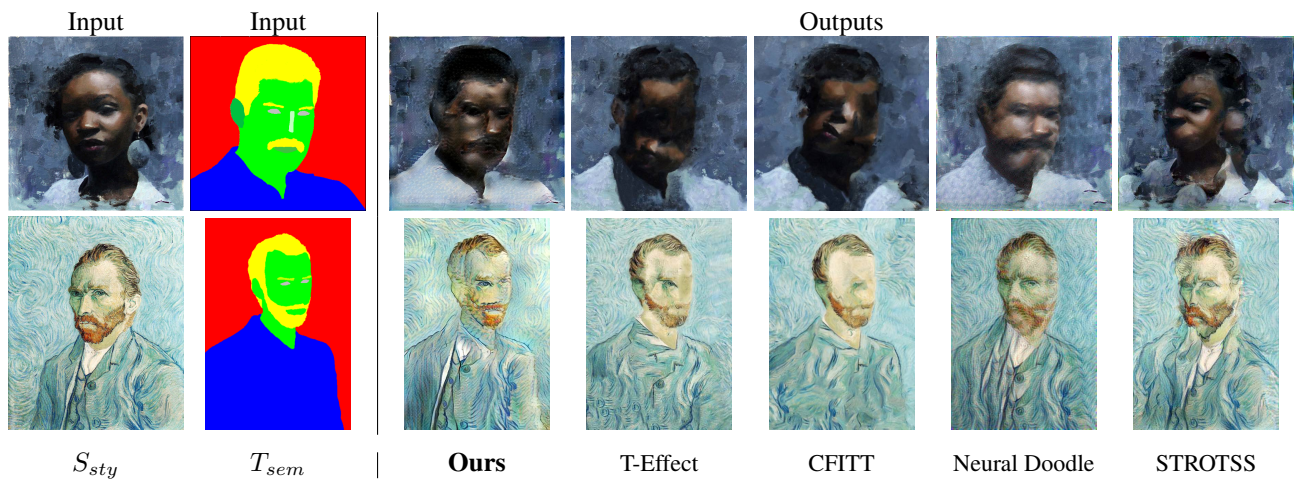


Figure 24: **Limitation of type 2: semantic maps with drastically different shapes.** Since our framework does not make patches rotated or scaled, it may not work very well for semantic maps with drastically different shapes (e.g., flipped poses). Nonetheless, as we can see, our method still outperforms SOTA in this situation. The issues may be solved by allowing patches to be rotated and scaled in our framework.

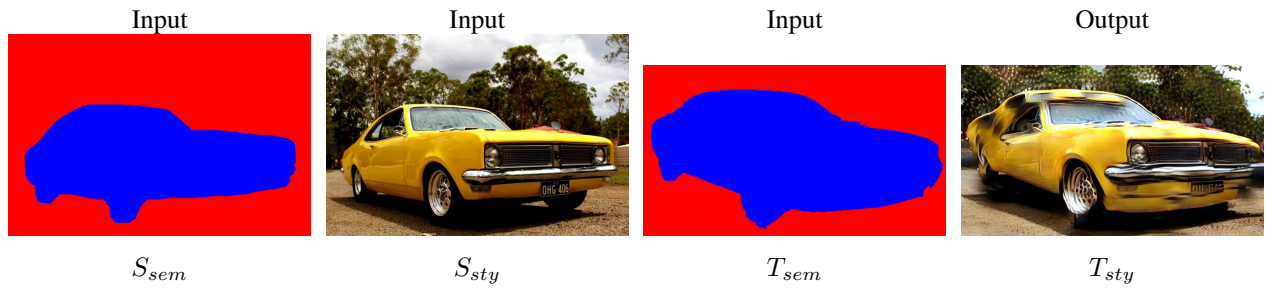


Figure 25: **Limitation of type 3: geometric texture transfer.** Our method cannot produce geometric texture transfer for images with strict structure requirements (e.g., the structures of the car shell and tires), because our VSTR does not allow patches to be either rotated or scaled. This issue may be addressed by allowing patches to be rotated and scaled in our framework, or using some geometric transformations like thin-plate spline interpolation (TPS) in the pipeline. Moreover, one may also model a deformation field like (Liu, Lin, and Hays 2004), or borrow some ideas from recent geometric style transfer approaches (Kim et al. 2020; Liu, Yang, and Hall 2021) to achieve geometric texture transfer.

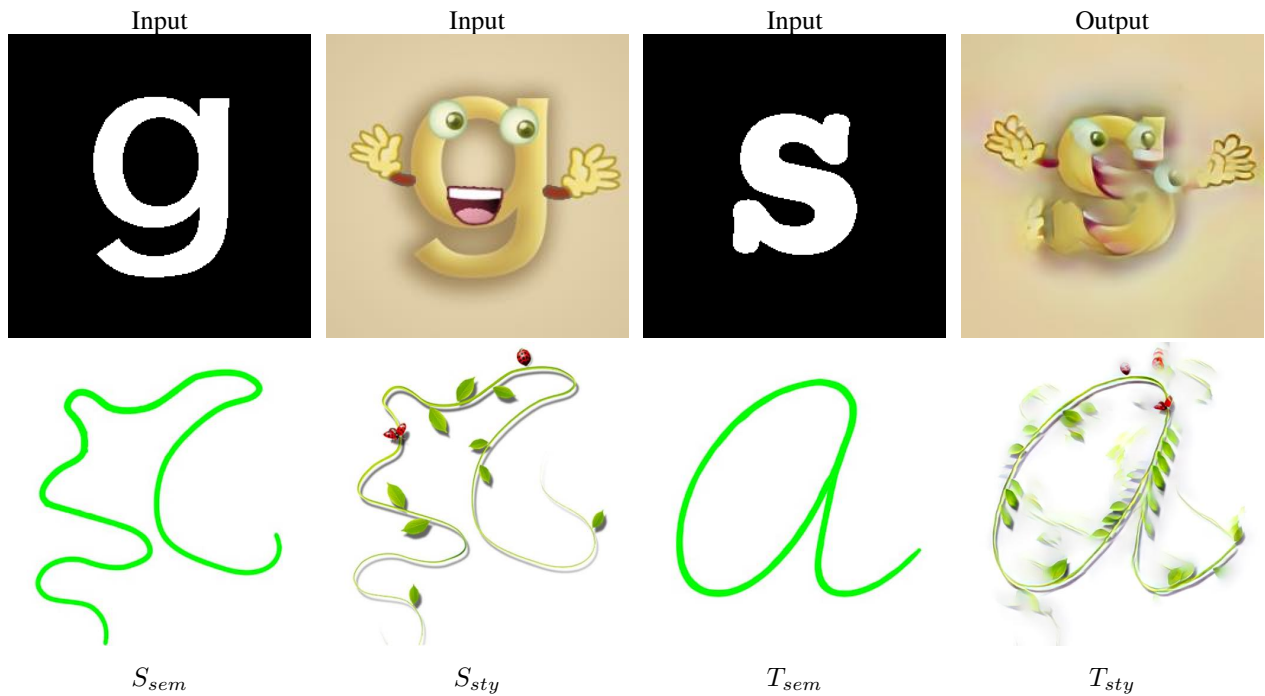


Figure 26: **Limitation of type 4: patterns with decorative elements.** Since our method does not use any additional structure guidance or distribution constraint, it may fail to achieve correct texture transfer for patterns with decorative elements (e.g., the eyes, mouth, and hands in the top row) when given extremely simple semantic maps. This may be solved by integrating additional guidances or distribution constraints like (Men et al. 2018) and (Yang et al. 2017), or simply specifying more elaborate semantic maps.